Electrode-tissues interface: Modelling and acute experiments on dogs

Y. Laaziri[1], F. Mounaim[1], E. Elzayat[2], M. Sawan[1], M.M. Elhilali [2]

[1] Polystim Neurotechnologies Laboratory, Department of Electrical engineering
Ecole Polytechnique de Montreal, Montreal, (QC) H3C 3A7, Canada
[2] Department of Urology
McGill University, Montreal, (QC) H3A 1A1, Canada

yassir.laaziri@polymtl.ca
http://www.polystim.polymtl.ca

Abstract

In this paper, we propose an empirical model for the Electrode-Tissues Interface (ETI). The model was validated by in vivo impedance measurements of the contact between cuff electrode and sacral nerves (S1-3) in four acute dog experiments for a frequency range of 1 Hz to 100 kHz. The results demonstrate a closer fitting between our proposed model and experimental measurements. Application of such model would allow us to have an accurate estimation of ETI impedance variation during nerve stimulation or Electroneurogram (ENG) recording.

1. INTRODUCTION

In biomedical engineering, electrode-tissues interface (ETI) behaviour is a major concern in implantable stimulators. To avoid any damage of living tissues, the interface interactions must be understood in order to insure a continuous and safe transfer of charges between the electrodes and tissues. Cuff electrodes are widely used for nerve stimulation and monitoring. The understanding of their overall behavior as well as processes undergoing at the ETI become important. Several models describing this ETI were proposed. Researchers focused on nonlinearity [1,2], Faradic current measurements [3] and ETI parameters variation in very low frequencies [4]. Unfortunately most of these models are limited to particular conditions such as stimulation parameters, biological environment and electrode types. In addition, the DC current flowing through the interface is rarely taken into account, and the effective contact area representing the electrode irregularity is often omitted.

In the present work, we propose an improved empirical model for the ETI, which takes into account most of the processes involved at that interface such as diffusion, stimulation current variation and effective contact area. However, we omitted the impurities of electrode materials and the electrode capacitance due to its negligible values. The proposed model is described in the next section and elaborated in section 2. Experimental results are presented and discussed in section 3, and conclusion in section 4.

2. DESCRIPTION OF THE ETI MODEL

A typical electrode-tissues contact is shown in Fig. 1a. Model of this interface includes two ETIs connected by an electrolytic resistance R_{el} in series with an electrode potential $E_{i=0}$. R_{el} is used to take into account the electrolyte resistance of the tissue. $E_{i=0}$ was cancelled by using the same materials, and the same area for the two contacts.

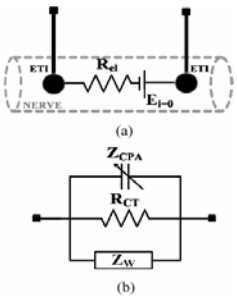

Figure 1: Electrode-tissues interface (ETI) model: (a) System of two contacts model, (b) ETI model. Z_{CPA} is the constant phase angle, R_{CT} a charge transfer resistance and Z_W the Warburg impedance, R_{el} represents the nerve resistance, $E_{i=0}$ is the standard electrode potential ($E_{i=0} = E_{1i=0} - E_{2i=0}$).

The typical ETI model is composed of a parallel combination of three main components (Fig. 1b): a non faradic pseudo capacitance (Z_{CPA}), a charge transfer resistance (R_{CT}) and the Warburg impedance (Z_w). These components take into account respectively the effective area of contact, the exchange current at the interface and the concentrations of carriers. Also, Z_{CPA} indicates the inhomogeneous area of contact:

$$Z_{CPA} = \frac{1}{(j\omega C_{dl})^{\beta}} \quad (1)$$

where ω is the angular frequency (s^{-1}) and β is a measure of the deviation from a pure capacitance. It is a significant parameter for ETI linearity [4]. C_{dl}, the double layer capacitance, represents the repartition of charge on both sides of the interface. On the other hand, R_{CT} corresponds to the exchanged current near the ETI. It is derived from the Butler-Volmer equation [4], which is required in order to take into account the DC current through the interface. It is function of stimulation current magnitude and the voltage across the interface. The third component, Z_w represents the diffusion of ionic species at the interface:

$$Z_w = \frac{\sigma}{\sqrt{\omega}}(1 - j) \quad (2)$$

where σ is the diffusion coefficient [5], which depends on the effective contact area, and the ion specie concentrations of oxidation-reduction reactions near the interface. For in vitro test, the tissues were replaced by NaCl 0.9 % solution, and R_{el} is replaced by ohmic resistance R_Ω, it is function of the electrolyte conductivity κ and the geometry of the electrode.

2. METHODS

Experimental results were collected from four adult male dogs. The contact between one cuff electrode and sacral nerve S2 was selected as the ETI. We monitor the ETI impedance using a commercially impedance-meter (LCR 3522 HIOKI). The meter measures the impedance magnitude with an accuracy of 0.08 % and impedance phase with an accuracy of 0.05 %.
The electrode, fabricated in our laboratory, consists of two stainless-steel leads covered with Teflon and soldered to two Platinum contacts [5]. The spacing between the electrodes is 5 mm and each contacts area is $4mm^2$. Sacral nerve S2 was placed inside the cuff, and the impedance magnitude and phase were measured for a range [1 Hz – 100 kHz] of frequencies. Impedance measurements were repeated for different stimulation current magnitudes (10 μA, 50 μA and 500 μA).

3. RESULTS

Fig. 2 depicts the measured impedance amplitudes and phases for different stimulation currents (10 μA, 50 μA and 500 μA) of the ETI, where the circles represent the experimental measurements. The continuous curve shows the results of theoretical impedance. All curves have a semilogX scale representation.

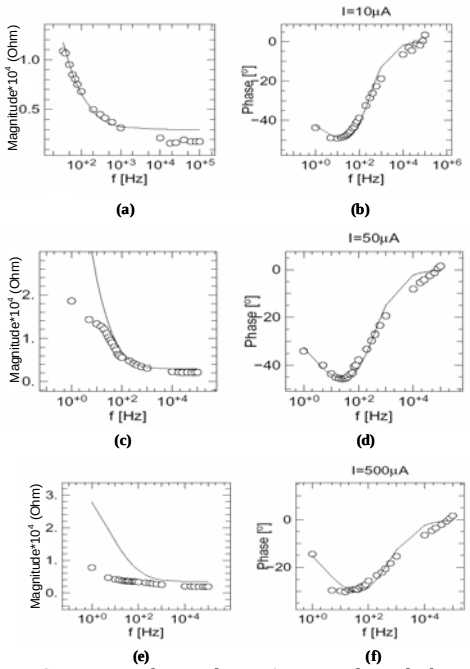

Figure 2: Measured impedance (magnitude and phase) of the ETI {nerve S2 - cuff electrode}: a,b) I_{stim} = 10 μA, c,d) I_{stim} = 50 μA, e,f) I_{stim} = 500 μA.

Figures 2a, 2c and 2e illustrate that ETI magnitudes decrease exponentially with frequency. The phase curve in Figures 2b, 2d and 2f shows resonance at 100 Hz under a stimulation current of 10 μA. This resonance increases with the stimulation magnitude. The model parameters are estimated from the impedance phase measurements, and then applied to the impedance magnitude curve. This is the reason why the phase theoretical curves match perfectly with measurements. In addition, the magnitude matches reasonably at high or low frequencies depending on the stimulation current magnitude. Measurement errors at very low frequencies may explain artefacts, resulting essentially from electrode polarization effect. Indeed, the accumulation of ions in the electrode is critical because of extended stimulation period. When frequency increases, the impedance magnitude decreases and tends to its lower limit that corresponds to the electrolyte resistance R_{el}.

Fig. 3 displays an experimental curve that shows the correlation between the ETI impedance and the stimulation current (I_{stim}). This correlation is relative to the charge transfer resistance R_{CT}. As I_{stim} increases, the magnitude and phase impedance decrease. For frequencies

higher than 100 kHz, the magnitude stabilizes and its phase is cancelled out. This confirms that R_{CT} is non linear compared to Z_{CPA} and it dominates the behavior of the ETI at very low frequencies, as it was reported in [1, 2, 3].

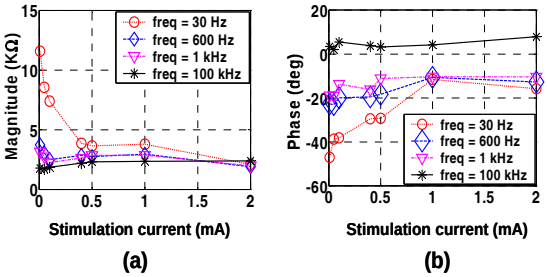

Figure 3: ETI impedance versus stimulation current: a) magnitude, b) phase.

The drawback is the presence of an undesirable shift in the impedance magnitude at very low frequencies. The lower the frequency, the more non linear R_{CT} becomes and the voltage across the interface increase At high frequency (above 10 kHz), the ETI behaves as resistor. Also at a given frequency, the decrease in the stimulation current and increase of the nerve diameter cause this resistor to increase. In order to improve the model, optimization software is used to fit theoretical impedance modeling with the experimentally measured variation (Fig. 2). For each stimulation current used in our experimental measurements, empirical values of our model parameters (R_{el},σ,R_{CT},C_{dl}) are estimated as summarized in Table 1.

Table 1: Experimental parameters that fit with the ETI model in different magnitudes of stimulation current.

Component		R_{el} (kΩ)	R_{CT} (kΩ)	σ ($\Omega/s^{1/2}$)	C_{dl} (nF)	β
I_{stim} (μA)	**10**	2.09	605.2	67082	731.3	0.95
	50	2.9	185.6	66466	603	0.95
	500	3.479	36.12	44369	415.2	0.95

As in vitro tests, we characterized the ETI by immersing cuff electrode into physiological saline solution (NaCl 0.9%). We made the same impedance measurements in order to compare the in vitro results with those of the acute measurements and calculate model parameters. Fig. 4 depicts a comparison between in vivo and in vitro measurements as well as the ETI model corresponding to these measurements. This comparison demonstrates the presence of R_{el} in the proposed ETI model. In fact, the contact with nerve is less capacitive than in physiological solution, which confirms that the ion concentrations are weak at the nerve-electrode interface.

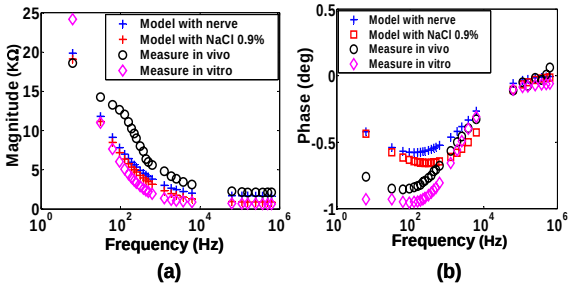

Figure 4: Comparison between in vivo and in vitro measurements: a) magnitude, b) phase.

4. CONCLUSIONS

We present in this work a general model of electrode-tissues interface which involved the major process at the ETI. We validate our proposed model with acute dog experiments. Moreover, we confirmed that R_{CT} is the main cause of ETI variations at very low frequencies. Thus, we concluded that for each magnitude of stimulation current, we have an optimum value of each ETI model component.

References

[1] McAdams, E.T., Lackermeier, A., McLaughlin, J.A., Macken, D., Jossinet, J., "The linear and non linear electrical properties of the electrode-electrolyte interface", *Biosensors and Bioelectronics*, Vol.10, pages: 67-74, 1995.

[2] Geddes, L.A., Roeder, R., "Measurement of the Direct-Current (Faradic) Resistance of the Electrode-Electrolyte interface for commonly used electrode materials", annals of biomedical engineering, Vol 29, pp.181-186, 2001.

[3] Richardot, A., McAdams, E.T., "Harmonic analysis of low frequency bioelectrode behavior", IEEE transactions on medical imaging, Vol.21, No.6, Pages: 604–612, 2002.

[4] Bard, A.J., Faulkner, L.R., "Electrochemical methods: fundamentals and applications", *John Wiley &sons*, 2nd edition, *A Wiley- Interscience Publication*, 820 pages, 2001.

[5] Crampon, M.A., Sawan, M., Brailovski, V., Trochu, F., **"**New nerve cuff electrode based on a shape memory alloy armature", proceedings of the 20th annual international conference of the IEEE EMBS, vol: 5, 29, 1998.

Acknowledgements

The authors acknowledge the financial support from the Canadian Institutes for Health Research (CIHR), and M.P. Bombardier for the electrode fabrication.